Discovery of novel histidine-derived lipo-amino acids: Applied in the synthesis of ultra-short antimicrobial peptidomimetics having potent antimicrobial activity, salt resistance a...

ARTICLE *in* EUROPEAN JOURNAL OF MEDICINAL CHEMISTRY · JULY 2013

Impact Factor: 3.45 · DOI: 10.1016/j.ejmech.2013.07.008 · Source: PubMed

European Journal of Medicinal Chemistry 68 (2013) 10–18

Contents lists available at ScienceDirect

European Journal of Medicinal Chemistry

journal homepage: http://www.elsevier.com/locate/ejmech

Original article

Discovery of novel histidine-derived lipo-amino acids: Applied in the synthesis of ultra-short antimicrobial peptidomimetics having potent antimicrobial activity, salt resistance and protease stability

Mija Ahn [a,1], Ravichandran N. Murugan [a,1], Binu Jacob [d,1], Jae-Kyung Hyun [b,1], Chaejoon Cheong [a], Eunha Hwang [a], Hyo-Nam Park [b], Ji-Hyung Seo [a], G. Srinivasrao [a], Kyung S. Lee [c], Song Yub Shin [d,**], Jeong Kyu Bang [a,*]

[a] Division of Magnetic Resonance, Korea Basic Science Institute, Ochang, Cheongwon, Chung-Buk 363-883, Republic of Korea
[b] Division of Electron Microscopic Research, Korea Basic Science Institute, 113 Gwahanno, Daejeon 305-333, Republic of Korea
[c] Laboratory of Metabolism, Center for Cancer Research, National Cancer Institute, National Institutes of Health, Bethesda, MD 20892, USA
[d] Department of Bio-Materials, Graduate School and Department of Cellular & Molecular Medicine, School of Medicine, Chosun University, Gwangju 501-759, Republic of Korea

ARTICLE INFO

Article history:
Received 29 May 2013
Received in revised form
16 July 2013
Accepted 18 July 2013
Available online 26 July 2013

Keywords:
Histidine-derived amino acid
Antimicrobial peptidomimetics
Salt resistance
Anti-MRSA activity
Protease stability

ABSTRACT

Here we report for the first time the synthesis of Histidine (His) derived lipo-amino acids having pendant lipid tails at $N(\tau)$- and $N(\pi)$-positions on imidazole group of His and applied it into synthesis of lipo-peptides. The attachment of His-derived lipo-amino acid into the very short inactive cationic peptides endows potent antimicrobial activity against Gram-positive and Gram-negative bacteria without hemolytic activity. Furthermore, our designed His-derived lipo-peptidomimetics (HDLPs) consisting of two or three residues displayed strong anti-MRSA activity and protease stability as well as retained potent antimicrobial activity under high salt concentration. Our results demonstrate that the novel lipo-amino acid is highly flexible to synthesize and carry out the extensive structure–activity relationship (SAR) on lipo-antimicrobial peptidomimetics and represents a unique amenable platform for modifying parameters important for antimicrobial activity. Through this study, we proved that the discovery of His-derived lipo-amino acid and the corresponding HDLPs are an excellent candidate as a lead compound for the development of novel antimicrobial agents.

1. Introduction

Most of all organisms have antimicrobial peptides (AMPs) as a defense system against invading pathogens. The AMPs have considerable attention as new antibiotics because of their potent broad-spectrum antimicrobial activity and rapid action. It makes bacteria more difficult to acquire resistance to AMPs compared to conventional antibiotic therapies [1–3]. Among them, lipo-peptides are an important class of AMPs because daptomycin and polymyxin have been already successfully evaluated in the clinics. Both daptomycin and polymyxin are formed by dual composition as such the cyclic peptide scaffolds and fatty acid residues of C_{14}–C_{18} length that are known to be integral to their activities [4,5]. In recent years, several groups reported that fatty acid attachment of cationic linear peptides endows inactive cationic peptides with antimicrobial activity. These lipo-peptides are generally composed of aliphatic acids attached to the *N*-terminus of cationic linear or cyclic peptides which displayed broad activity against both Gram-positive and Gram-negative bacteria [6–15]. In addition, the higher hydrophobicity gained through fatty acid attachment can be considered as a useful remedy for the salt sensitive peptide binding that limits the bacterial potency at physiological ionic strength [16]. However, a potential downside of these lipo-peptides is their high production cost due to large size which doesn't allow large scale synthesis and the decrease in water solubility due to lipidation that can have severe pharmacokinetic consequences. In addition, there are limitations on the bioavailability of lipo-peptides since they can be easily degraded by the peptidase like trypsin owing to multiple Arg or Lys residues.

* Corresponding author. Tel.: +82 43 240 5023; fax: +82 43 240 5059.
** Corresponding author. Tel.: +82 62 230 6769; fax: +82 62 233 6337.
E-mail addresses: syshin@chosun.ac.kr (S.Y. Shin), bangjk@kbsi.re.kr (J.K. Bang).
[1] These authors contributed equally to this work.

0223-5234/$ – see front matter © 2013 Elsevier Masson SAS. All rights reserved.
http://dx.doi.org/10.1016/j.ejmech.2013.07.008

Herein, we focused on developing the short Histidine-derived lipo-peptidomimetics (HDLPs) as a new class of lipidated peptidomimetics having ultra-short length (2 or 3 residues) by modulating the charge, hydrophobicity and amphipathicity. This is the critical issue for the therapeutic development of AMPs, since the long peptide sequence of AMPs, typically having 10–50 amino acids, limits their use in systematic administration and biological uptake [17]. Thus, if AMPs potency and selectivity can be retained for short HDLPs, it would open up new avenues for the wider pharmaceutical applicability of antimicrobial peptidomimetics. To achieve this goal, we have developed a pendant alkyl-tagging on Histidine (His) amino acid with hydrophobic groups stretches as a key residue for the facile and readily tunable approach to increase the lipophilicity [18,19]. The solid-phase synthesis of HDLPs is straightforward, and their potential diversification is large by the introduction of a variety of functional groups.

In this study we modified the short HDLPs by positioning from *C*- to *N*-terminus with His residue that was lipidated on the side chain of imidazole group. Until now, this strategy has been rarely employed: usually *N*-terminal lipidation is performed to investigate structure–activity study on antimicrobial peptides. In order to identify the most promising, cost-effective ultra-short AMPs as a drug candidate, our designed HDLPs were compared in terms of (i) broad-spectrum of antimicrobial activity, (ii) prokaryotic selectivity, (iii) anti-MRSA activity, (iv) proteolytic stability and (v) salt resistance.

2. Results and discussion

2.1. Design and synthesis

The design of the 8 HDLPs is based on the fact that a global distribution of cationic and hydrophobic side chains is a key to antimicrobial activity, which can be easily constructed by attaching aliphatic alkyl tail to cationic peptide. The synthesis of HDLPs was carried out on solid phase and characterized by HPLC and MALDI-TOF Mass. Fmoc-His(Trt)-OH was used as a starting material to synthesize the lapidated His derivatives as a building blocks. As a first step, Fmoc-His(Trt)-OH was coupled with the excess of methanol in the presence of *N*-(3-dimethylaminopropyl)-*N*′-ethylcarbodiimide hydrochloride (EDCI) and 1-hydroxybenzotriazole (HOBt) to carry out the esterification reaction. Then, the $N(\tau)$- and $N(\pi)$-positions on Fmoc-His(Trt)-OMe were dialkylated using alkyl or alkenyl alcohols in the presence of triflic anhydride and diisopropylethylamine (DIEA), followed by the treatment of trifluoroacetic acid (TFA) and triisopropylsilane (TIS) for 2 h at room temperature. Finally, lapidated Fmoc-protected His derivatives were obtained in good yield through hydrolysis of ester (Scheme 1). Next, the above synthesized $N(\tau)$-alkyl, $N(\pi)$-alkyl bis-adducted His monomers were successfully used to generate our focused peptidomimetic derivatives using Rink amide resin by the conventional solid phase peptide synthesis (Scheme 1 and Fig. 1).

Our focused HDLP derivatives contain variety of lipophilic acids including saturated C_7-, C_{10}-, and C_{14}-, and an unsaturated lipid moiety in order to study how chain length and aggregation (saturation vs unsaturation) of the lipophilic moiety affects the antimicrobial activity. For example, HDLP1–3 are cationic lipo-peptidomimetics having either C_7, C_{10}, or C_{14} as pendant alkyl at $N(\tau)$-, $N(\pi)$-position, respectively. HDLP4 containing $N(\pi)$ mono-alkylated tail was generated to see the effect of hydrophobicity on antimicrobial activity compared to HDLP2. HDLP5 having same sequence with HDLP4 but with unsaturated lipid tail was derived to see the effect of unsaturation on increasing the potency of antimicrobial activity by limiting the aggregation of peptides. HDLP6 and HDLP7 were generated to investigate the positional effect on antimicrobial activity by moving alkyl tail from center (HDLP2) to *N*-terminal (HDLP6) and *C*-terminal (HDLP7), respectively. Finally, to understand the role of charge on HDLP2 in the antimicrobial activity, we derived dimeric peptide HDLP8 by the *N*-terminal deletion of Arg and analyzed the antimicrobial activity (Fig. 1).

2.2. Antimicrobial and hemolytic activities

All of the peptides were assayed for their antimicrobial activities towards three Gram-negative bacteria (*Escherichia coli*, *Pseudomonas aeruginosa* and *Salmonella typhimurim*) and three Gram-positive bacteria (*Staphylococcus epidermidis*, *Bacillus subtilis* and *Staphylococcus aureus*). The cytotoxicity of the peptides was evaluated by testing hemolysis with human red blood cells (hRBCs). For the purpose of comparison, the previously reported active AMPs, human cathelicidin LL-37 and bee venom melittin, were served as a positive control for antimicrobial and hemolytic activities.

Our assay results demonstrated that ultra-short HDLPs appear to be very effective and a novel class of antimicrobial agents. As shown in Table 1, almost all the HDLPs except HDLP3 displayed potent antimicrobial activity (average MIC range: 3.7–24.0 μg/ml) against Gram-positive and Gram-negative bacteria. The HDLP1 bearing two Arg residues and one His derivative which has C_7 alkyl tail at $N(\tau)$-, $N(\pi)$-position, displayed one of the most potent antimicrobial activity with the MIC value 2–8 μg/ml against all bacteria tested. Particularly, the activity of HDLP1 displayed the same or little higher activity compared with melittin which was known to possess the strong antimicrobial activity. The therapeutic potential of peptide antimicrobial drugs lies in their prokaryotic selectivity to effectively kill bacterial cells without exhibiting significant cytotoxicity toward mammalian cells such as hRBCs. To determine prokaryotic selectivity of the peptides, we calculated their therapeutic index (TI) (Table 1). The TI is a widely employed parameter to represent the prokaryotic selectivity of antimicrobial agents. The TI of the peptides is calculated as the ratio of the HC_{50} to GM (geometric mean of MICs against six bacterial strains); thus, larger values of TI indicate greater prokaryotic selectivity. When there was no hemolysis at the highest concentration tested (256 μg/ml), 512 μg/ml was used for the TI calculation, since the test was carried out by two-fold serial dilution. HDLP1showed the highest TI value among our designed HDLPs. HDLP1 displayed almost 70 times higher TI value in comparison to melittin, which augments its potential development as antimicrobial agents to treat both Gram-negative and Gram-positive bacterial infections (Table 1 and Fig. 2).

Next, to investigate the effect of length of alkyl tail on antimicrobial activity, we designed and synthesized HDLP2 and HDLP3 having either C_{10} or C_{14} as pendant alkyl tail, respectively (Fig. 1). Since antimicrobial activity is positively correlated with hydrophobicity, we expected that HDLP2 and HDLP3 display more potent antimicrobial activity than HDLP1 because of increasing the hydrophobicity by extending the alkyl tail length. As shown in Table 1, changing the alkyl tail length from C_7 (HDLP1) to C_{10} (HDLP2) did not alter the antimicrobial activity even though hemolytic activity was increased (Fig. 2). Against expectations, HDLP3 having the highest hydrophobic properties among the HDLPs series due to the presence of C_{14} as pendant alkyl tail completely lost its antimicrobial activity and reduced its hemolytic activity (Table 1). It is possible that there is an optimum length of lipophilic tail for HDLP activity or lipophilicity of the HDLP is self-limiting due to aggregation or an unknown mechanism.

On the basis of above results, further evaluation was carried out to see the effect of hydrophobicity by replacing dialkylated HDLP2 to $N(\pi)$-mono-alkylated peptide, HDLP4 (Fig. 1). The assay results showed that the hydrophobicity played an important role in antimicrobial activity against Gram-negative bacteria because all the strains showed 2–4 fold decreased activity compared to HDLP2. On the other hand, the Gram-positive bacteria were insensitive to

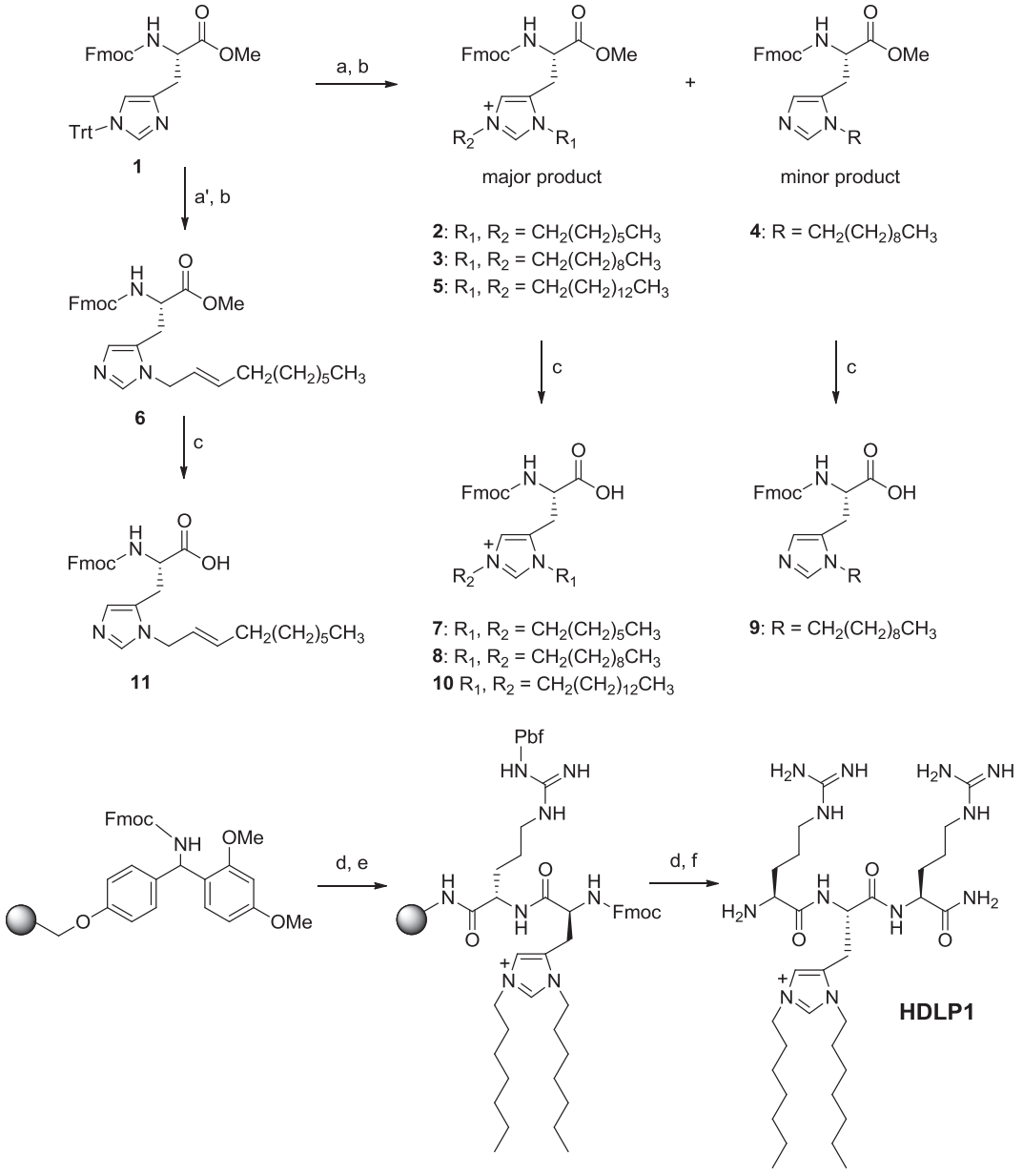

Scheme 1. Synthetic protocol of Fmoc-His-OH derivatives and trimeric HDLP1 using solid phase peptide synthesis (SPPS): (a) R-OH (2.2 eq.), Tf_2O (2.2 eq.), DIEA (2.2 eq.), CH_2Cl_2, −78 °C–rt, 15 h. (a′) *trans*-2-decen-1-ol (1.1 eq.), Tf_2O (1.1 eq.), DIEA (1.1 eq.), CH_2Cl_2, −78 °C–rt, 15 h. (b) TFA (10 eq.), TIS (1.1 eq.), CH_2Cl_2, rt, 2 h. (c) 2 N HCl-1,4-dioxane (1:1), reflux, 10 h. (d) i. 20% piperidine in DMF, 15 min. ii. Fmoc-Arg(pbf)-OH, HBTU, HOBt, DIEA, DMF, 1 h. (e) i. 20% piperidine in DMF, 15 min. ii. **7**, HBTU, HOBt, DIEA, DMF, overnight. (f) i. 20% piperidine in DMF, 15 min. ii. TFA/TIS/H_2O (90:5:5), 2 h.

change in hydrophobicity (Table 1). We also designed and synthesized the HDLP5, having identical sequence to HDLP4 but contains unsaturated lipophilic tail at *N*(π) position and assayed its antimicrobial activity. But, the 2-fold decreased in antimicrobial activity of HDLP5 against HDLP4 suggests that the unsaturated lipophilic tail on HDLPs may not enhance the potency of antimicrobial activity (Fig. 1 and Table 1).

An important, yet rarely explored in various studies, question is how the activity of the amphiphilic HDLPs varies as a function of spatial positioning of the positive charge and lipophilic pendant alkyl tail [20]. Since our HDLPs are very unique by having lipophilic tail at the middle of the sequence, we focused to study the influence of spatial positioning of the hydrophobic alkyl tail on antimicrobial activity by incorporating either at the *N*-terminus (HDLP6) or *C*-terminus (HDLP7) from the middle (HDLP2). The assay result showed that there was no appreciable change on the antimicrobial activity by both *N*-terminal and *C*-terminal segregation of hydrophobic alkyl tail when compared to the HDLP2 (Fig. 1 and Table 1). This result demonstrated that antimicrobial activity was less sensitive to the spatial positioning of the lipophilic tail.

Finally, to understand the role of charge on HDLPs in the antimicrobial activity, we synthesized dimeric peptide HDLP8 by the *N*-terminal deletion of Arg and analyzed the antimicrobial activity. Being very short lipidated HDLP, HDLP8 surprisingly displayed similar activity against Gram-negative bacteria and even more active against Gram-positive bacteria compared to trimeric HDLP2 (Fig. 1 and Table 1). This indicates that lipophilicity of the pendant alkyl tail on HDLPs was critical and the decreased cationic property by the deletion of Arg at the *N*-terminus did not affect the antimicrobial activity, but induced almost 2-fold decrease in the TI value due to

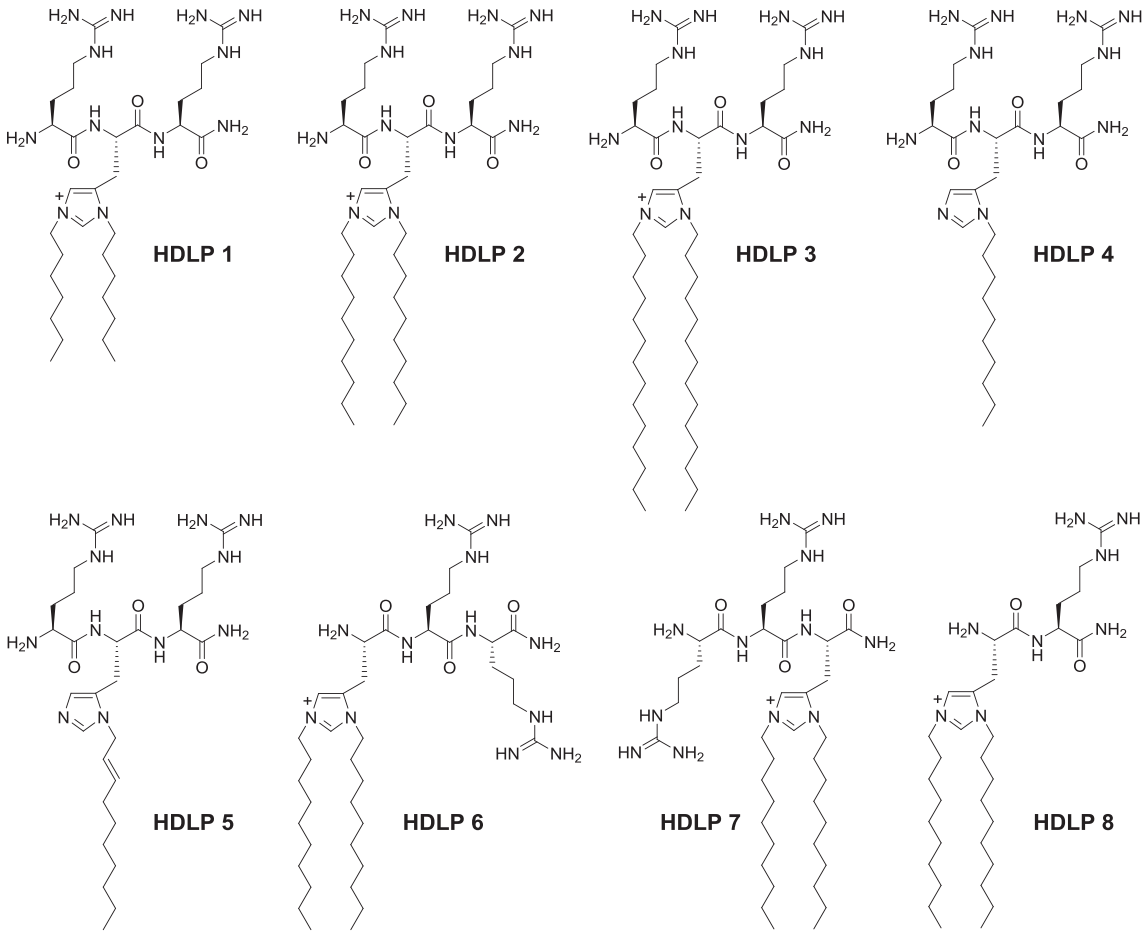

Fig. 1. The structures of HDLPs tested for their antimicrobial activity.

increase in hemolytic activity. To the best of our knowledge, HDLP8 is one of most short lipo-peptidomimetics having potent broad-spectrum antimicrobial activity.

2.3. Anti-MRSA activity

Next, we tested the antimicrobial activity of our designed HDLPs against methicillin-resistant *S. aureus* (MRSA). The annual frequency of deaths from MRSA, a major cause of skin and soft-tissue infections in the hospital, is rapidly increasing and has greater than those caused by human immunodeficiency virus/acquired immune deficiency syndrome (HIV/AIDS) [21]. Hence, in addition to the above broad-spectrum activity study, MRSA strains (MRSA 1, 2, and 3) were employed as a multi-drug resistant bacteria. Surprisingly, most of our HDLPs (1, 2, 4, 5, 6, 7 & 8) were found to retain the activity against the methicillin-resistant strains whereas HDLP3 didn't showed the any activity against MRSA strains tested (Table 2).

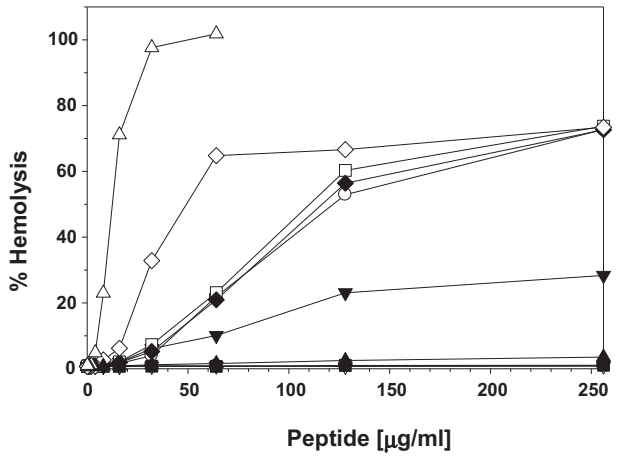

Fig. 2. Concentration-response curves of percent hemolysis of the peptides against human red blood cells. Peptides are indicated as follows: HDLP1 (●), HDLP2 (○), HDLP3 (▼), HDLP4 (▽), HDLP5 (■), HDLP6 (□), HDLP7 (◆), HDLP8 (◇), LL-37 (▲), melittin (△).

2.4. Salt resistance

The salt sensitivity of AMPs is a major obstacle in their development as novel therapeutic agents. It was well known that the electrostatic attractions between AMPs and bacterial membranes at high ionic strength showed reduced driving force for AMP adsorption and in partial or complete loss in antimicrobial activity at physiological conditions. Salt sensitivity has been observed in several AMPs including α-defensins, and cecropins [22]. For effective use in clinical pharmacotherapy, AMPs need to remain active in the presence of physiological levels of salt (150 mM NaCl). For this reason, we tested the effects of NaCl on antimicrobial activity of our designed HDLPs against six bacterial strains. As shown in Table 3, HDLPs 2, 6, 7 and 8 appeared to be relatively resistant to NaCl concentration of 150 mM. In contrast, HDLPs 1, 3, 4 and 5 showed a drastic increase in their MIC values in the presence of 150 mM NaCl.

Table 1
Antimicrobial and hemolytic activities and therapeutic index of the designed peptides.

Peptides	Minimal inhibitory concentration (MIC) (μg/ml)						GM[a] (μg/ml)	HC_{50}[b] (μg/ml)	TI[c] (HC_{50}/GM)
	E. coli [KCTC 1682]	*P. aeruginosa* [KCTC 1637]	*S. typhimurium* [KCTC 1926]	*S. epidermidis* [KCTC 1917]	*B. subtilis* [KCTC 3068]	*S. aureus* [KCTC 1621]			
HDLP1	4	8	8	2	2	4	4.7	>256	108.9
HDLP2	8	8	8	4	4	4	5.3	121	22.8
HDLP3	>64	>64	>64	>64	>64	>64	128.0	>256	4.0
HDLP4	16	16	32	2	2	4	12.0	>256	42.7
HDLP5	32	32	64	4	4	8	24.0	>256	21.3
HDLP6	8	8	8	4	4	4	6.0	110	18.3
HDLP7	16	8	8	8	8	8	9.3	116	12.5
HDLP8	4	8	4	2	2	2	3.7	49	13.2
LL-37	32	64	16	16	32	32	32.0	>256	16.0
Melittin	8	8	8	8	4	4	6.7	10.5	1.6

[a] The geometric mean (GM) of the MIC values for four bacterial strains. When no detectable antimicrobial activity was observed at the maximum concentration (64 μg/ml), the value of twice maximum concentration (128 μg/ml) was used for calculation of the therapeutic index.
[b] HC_{50} is the peptide concentration that produces 50% hemolysis against human red blood cells. When no detectable hemolytic activity was observed at the maximum concentration (256 μg/ml), the value of twice maximum concentration (512 μg/ml) was used for calculation of the therapeutic index.
[c] Therapeutic index (TI) is the ratio of the HC_{50} value to the GM.

2.5. Protease stability

Another main drawback of AMPs into development of therapeutic applications is intrinsic instability by protease. Of great concern are trypsin-like proteases that abound in the body and are selective for basic residues. Trypsin specifically catalyzes the hydrolysis of *C*-terminal amide bonds of lysine and arginine [23]. Since our HDLPs possess one or two arginine residues, their proteolytic stability was examined by tryptic degradation. The HDLPs 1, 2, 4, 6, 7 and 8 having relatively high antimicrobial activity were pretreated with trypsin and their residual antimicrobial activity was assayed by the broth microdilution assay. All of our HDLPs tested preserved completely their antimicrobial activity against *E. coli* and *S. aureus* after trypsin treatment, while melittin and LL-37 partially or completely abolished their antimicrobial activity (Fig. 3).

2.6. Mechanistic studies using TEM

As a brief study of the mechanism of action, the effects of treating *E. coli* and *S. aureus* with HDLPs 1, 2, 6 and 7 were studied by transmission electron microscopy (TEM). In comparison to untreated control, obvious disruption of cellular structure was observed when HDLPs 1, 2, 6 and 7 were added (Fig. 4) in which clear rupturing of bacterial cells and release of internal materials were clearly visible.

3. Conclusion

In conclusion, three main findings are presented in this report. First, it shows the applicability of lipophilic tagging as a means for enhancing antimicrobial potency of ultra-short, highly cationic AMPs against Gram-positive and Gram-negative bacteria including MRSA strains. Second, the results indicate that the proteolytic stability is achieved by the precise addition of lipophilic tail on His imidazole ring, the latter being particularly sensitive to proteolytic inactivation. Third, the optimized HDLPs retained high antimicrobial potency at high NaCl ionic strength. Collectively, our findings demonstrated that the small amphipathic HDLPs may be a promising class of antimicrobial agents by means of having a similar range of antimicrobial potency and prokaryotic selectivity as larger cationic AMPs in addition to improved proteolytic stability, salt resistance and lower costs of production.

Table 2
Antimicrobial activity of the peptides against methicillin-resistant *Staphylococcus aureus* (MRSA) strains.

Peptide	Minimal inhibitory concentration (MIC) (μg/ml)		
	MRSA 1 (CCARM 3089)	MRSA 2 (CCARM 3090)	MRSA 3 (CCARM 3095)
HDLP1	4	8	4
HDLP2	8	4	4
HDLP3	>64	>64	>64
HDLP4	8	8	8
HDLP5	16	16	16
HDLP6	4	4	4
HDLP7	8	8	8
HDLP8	2	4	2
LL-37	>32	>32	>32

4. Experimental

4.1. General experimental

Reagents were obtained commercially (Sigma–Aldrich, TCI) and used without further purification. All reactions were carried out under nitrogen atmosphere in oven-dried glassware. CH_2Cl_2 was distilled under N_2 from CaH_2 immediately before use. Analytical TLC was performed on silica gel plate using UV light and/or ninhydrin stain followed by heating. Column chromatography was performed on silica gel 60 (230–400 mesh). ^1H and ^{13}C NMR spectra were obtained on a Bruker DRX 400 spectrometer at 400 and 100 MHz, respectively. Chemical shifts (δ) are reported in parts per million (ppm) measured relative to an internal standard, and coupling constants (J) are expressed in hertz (Hz). Mass spectra were obtained on a Waters SYNAPT G2 (ESI) mass spectrometer.

4.2. Synthesis of N(α)-[(9H-fluoren-9-ylmethoxy)carbonyl]-N(τ)-(triphenylmethyl)-L-histidine methyl ester (**1**)

To a solution of Fmoc-His(Trt)-OH (3.10 g, 5.00 mmol) in CH_2Cl_2 (30 mL) were added EDCI (1.05 g, 5.50 mmol), HOBt (743 mg, 5.50 mmol), and MeOH (1 mL, excess) at room temperature and stirred for 15 h. The mixture was diluted with CH_2Cl_2 and washed with H_2O. The organic layer was dried (Na_2SO_4) and evaporated in vacuo. The residue was purified by silica gel column chromatography (CH_2Cl_2/MeOH, 20:1) to provide **1** (3.0 g, 95%) as a white foam.

^1H NMR (400 MHz, $CDCl_3$): δ 7.75 (d, 2H, J = 7.5 Hz), 7.62 (t, 2H, J = 7.5 Hz), 7.53 (s, 1H), 7.42–7.26 (m, 13H), 7.13–7.10 (m, 6H), 6.57 (s, 1H), 6.53 (d, 1H, J = 8.2 Hz), 4.63 (m, 1H), 4.38–4.22 (m, 3H), 3.63 (s, 3H), 3.13–3.03 (m, 2H). ^{13}C NMR (100 MHz, $CDCl_3$): δ 172.0, 156.2, 144.1, 143.9, 142.2, 141.2, 138.8, 136.2, 129.7, 128.12, 128.09,

Table 3
Antimicrobial activity of the designed peptides in the presence of 150 mM NaCl.

Peptides	Minimal inhibitory concentration (MIC) (μg/ml)					
	E. coli [KCTC 1682]	*P. aeruginosa* [KCTC 1637]	*S. typhimurium* [KCTC 1926]	*S. epidermidis* [KCTC 1917]	*B. subtilis* [KCTC 3068]	*S. aureus* [KCTC 1621]
HDLP1	>32	8	32	16	8	8
HDLP2	16	8	16	4	4	4
HDLP3	>64	>64	>64	>64	>64	>64
HDLP4	>64	16	>64	32	8	32
HDLP5	>64	64	64	64	16	32
HDLP6	16	8	16	4	4	8
HDLP7	16	8	16	4	4	4
HDLP8	8	8	8	2	2	2
LL-37	16	64	32	>64	16	>64
Melittin	8	8	16	4	8	2

127.6, 127.1, 125.4, 125.3, 119.9, 119.7, 75.4, 67.2, 54.3, 52.2, 47.2, 33.9, 30.1.

All the values are in agreement with the reported values [24].

4.3. General procedure I for alkylation of histidine methyl ester **2**–**6**. The synthesis was performed in accordance to Qian et al. [24]

4.3.1. N(α)-[(9H-Fluoren-9-ylmethoxy)carbonyl]-N(π), N(τ)-bis(heptyl)-L-histidine methyl ester (**2**)

To a solution of triflic anhydride (877 μL, 5.21 mmol) in CH_2Cl_2 (35 mL) under nitrogen at −78 °C were added a solution of 1-heptanol (736 μL, 5.21 mmol) and DIEA (907 μL, 5.21 mmol) in CH_2Cl_2 (45 mL) dropwise over a 30 min and stirred for an additional 30 min. Subsequently, a solution of **1** (1.50 g, 2.37 mmol) in CH_2Cl_2 (20 mL) was added dropwise. After 10 min, the reaction mixture was slowly warmed to room temperature and stirred for 15 h. At 0 °C, satd. $NaHCO_3$ solution was slowly added to the reaction mixture and stirred for 30 min, and extracted with CH_2Cl_2. The organic extract was washed with brine and dried (Na_2SO_4), and evaporated in vacuo. To a solution of resulting product in CH_2Cl_2 (20 mL) were added TFA (1.81 mL, 23.70 mmol) and triisopropylsilane (535 μL, 2.61 mmol) and stirred at room temperature for 2 h. The solvent was removed in vacuo, and the residue was purified by silica gel column chromatography (CH_2Cl_2/MeOH, from 100:1 to 20:1) to provide **2** (1.08 g, 77%) as a colorless gum.

^{1}H NMR (400 MHz, $CDCl_3$): δ 8.96 (s, 1H), 7.73 (d, 2H, J = 7.5 Hz), 7.66–7.59 (m, 2H), 7.37 (t, 2H, J = 7.4 Hz) 7.33–7.28 (m, 3H), 6.73 (d, 2H, J = 8.0 Hz), 4.55 (m, 1H), 4.35–4.20 (m, 2H), 4.17 (m, 1H), 4.13–4.04 (m, 2H), 4.4.0–3.99 (t, 2H, J = 7.4 Hz), 3.77 (s, 3H), 3.33–3.17 (m, 2H), 1.86–1.75 (m, 2H), 1.74–1.64 (m, 2H) 1.33–1.09 (m, 16H), 0.89–0.76 (m, 6H). ^{13}C NMR (100 MHz, $CDCl_3$): δ 170.6, 156.2, 143.8, 143.5, 141.2, 135.7, 131.4, 127.8, 127.2, 127.1, 125.4, 125.3, 122.3, 120.4, 120.0, 119.1, 67.4, 53.0, 52.5, 50.0, 47.4, 46.9, 31.5, 31.45, 30.0, 29.9, 28.6, 28.5, 26.2, 26.0, 25.9, 22.5, 22.4, 14.0, 13.9. MS (ESI) m/z 588.3 (M).

4.3.2. N(α)-[(9H-Fluoren-9-ylmethoxy)carbonyl]-N(π), N(τ)-bis(decyl)-L-histidine methyl ester (**3**) and N(α)-[(9H-fluoren-9-ylmethoxy)carbonyl]-N(π)-(decyl)-L-histidine methyl ester (**4**)

Compound **3** and **4** were synthesized using general procedure I, Tf_2O (1.75 mL, 10.41 mmol), 1-decanol (1.99 mL, 10.41 mmol), histidine methyl ester **1** (3.00 g, 4.73 mmol), DIEA (1.81 mL, 10.41 mmol), TFA (3.63 mL, 47.34 mmol), and TIS (1.07 mL, 5.20 mmol). The crude product was purified by silica gel column chromatography (CH_2Cl_2/MeOH, from 100:1 to 20:1) to provide **3** (2.6 g, 82%) as a colorless gum and **4** (0.6 g) as a white foam.

Compound **3**: ^{1}H NMR (400 MHz, $CDCl_3$): δ 8.88 (s, 1H), 7.74 (d, 2H, J = 7.4 Hz), 7.62 (m, 2H), 7.39 (t, 2H, J = 7.4 Hz), 7.31 (t, 2H, J = 7.4 Hz), 7.13 (s, 1H), 6.50 (d, 1H, J = 7.7 Hz), 4.58 (m, 1H), 4.36 (m, 1H), 4.28 (m, 1H), 4.20 (t, 1H, J = 7.2 Hz), 4.13–4.02 (m, 4H), 3.79 (s, 3H), 3.25 (m, 2H), 1.80–1.71 (m, 4H), 1.27–1.22 (m, 28H), 0.87 (t, 6H, J = 6.7 Hz). ^{13}C NMR (100 MHz, $CDCl_3$): δ 170.6, 156.4, 143.8, 143.5, 141.2, 135.7, 131.4, 127.8, 127.17, 127.15, 125.5, 125.3, 122.3, 120.3, 120.0, 119.1, 67.5, 53.0, 52.5, 50.0, 47.4, 46.9, 31.8, 29.97, 29.91, 29.44, 29.43, 29.4, 29.36, 29.25, 29.23, 29.0, 28.9, 26.3, 26.1, 25.8, 22.6, 14.1. MS (ESI) m/z 672.5 (M).

Compound **4**: ^{1}H NMR (400 MHz, $CDCl_3$): δ 8.56 (s, 1H), 7.77 (d, 2H, J = 7.4 Hz), 7.57 (m, 2H), 7.41 (t, 2H, J = 7.4 Hz), 7.32 (t, 2H, J = 7.4 Hz), 7.15 (s, 1H), 5.90 (d, 1H, J = 7.3 Hz), 4.56 (m, 1H), 4.41 (m, 2H), 4.19 (t, 1H, J = 6.8 Hz), 4.01 (m, 2H), 3.79 (s, 3H), 3.13–3.25 (m, 2H), 1.79 (br s, 2H), 1.24–1.29 (m, 14H), 0.88 (t, 3H, J = 6.5 Hz). ^{13}C NMR (100 MHz, $CDCl_3$): δ 170.5, 156.0, 143.6, 143.5, 141.3, 134.7,

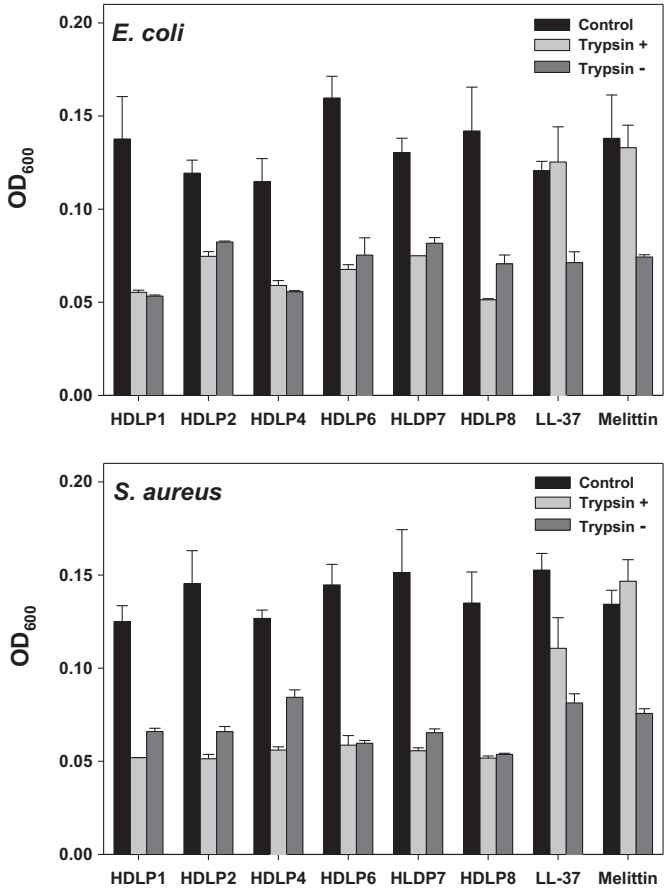

Fig. 3. Inhibition of antimicrobial activity of the peptides by trypsin assessed using the broth microdilution assay.

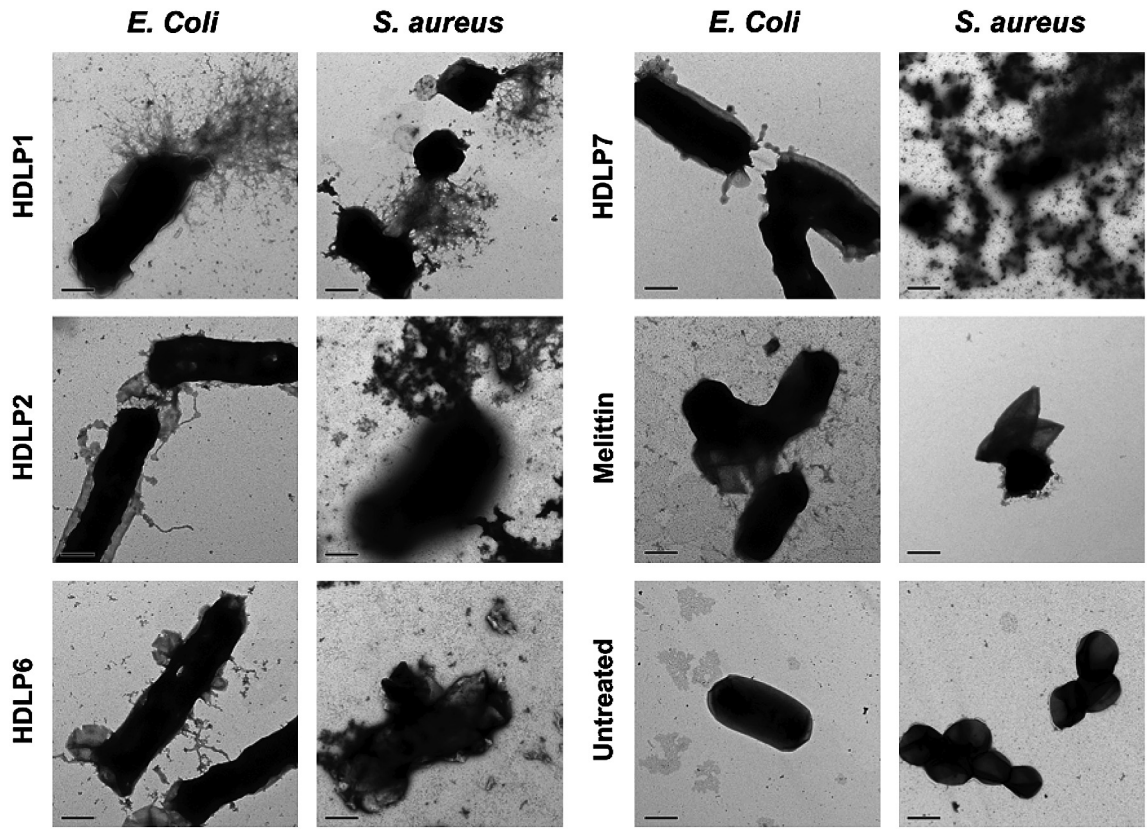

Fig. 4. Electron micrographs of negatively stained *E. coli* and *S. aureus* untreated or treated with HDLPs and melittin. All images are scaled, and the scale bar represents 1 μm.

129.4, 127.8, 127.1, 125.0, 120.0, 119.0, 67.3, 53.1, 52.9, 47.0, 46.9, 31.8, 30.1, 29.4, 29.3, 29.2, 28.9, 26.3, 26.1, 22.6, 14.1. MS (ESI) *m*/*z* 532.3 $(M + H)^+$.

4.3.3. *N(α)-[(9H-Fluoren-9-ylmethoxy)carbonyl]-N(π), N(τ)-bis (tetradecyl)-L-histidine methyl ester (**5**)*

Compound **5** was synthesized using general procedure I, Tf_2O (1.76 mL, 10.49 mmol), 1-tetradecanol (2.25 g, 10.49 mmol), histidine methyl ester **1** (3.02 g, 4.77 mmol), DIEA (1.83 mL, 10.49 mmol), TFA (3.65 mL, 47.66 mmol), and TIS (1.08 mL, 5.25 mmol). The crude product was purified by silica gel column chromatography (CH_2Cl_2/MeOH, from 100:1 to 20:1) to provide **5** (1.45 g, 39%) as a colorless gum and *N*(α)-[(9*H*-fluoren-9-ylmethoxy)carbonyl]-*N*(π)-(tetradecyl)-L-histidine methyl ester (0.69 g).

^{1}H NMR (400 MHz, $CDCl_3$): δ 8.92 (s, 1H), 7.74 (d, 2H, *J* = 7.4 Hz), 7.62 (m, 2H), 7.38 (t, 2H, *J* = 7.4 Hz), 7.30 (t, 2H, *J* = 7.4 Hz), 7.17 (s, 1H), 6.59 (br s, 1H), 4.57 (m, 1H), 4.34 (m, 1H), 4.26 (m, 1H), 4.18 (m, 1H), 4.13–4.00 (m, 4H), 3.78 (s, 3H), 3.25 (m, 2H), 1.80 (br s, 2H), 1.71 (br s, 2H), 1.25–1.18 (m, 44H), 0.88 (t, 6H, *J* = 6.5 Hz). ^{13}C NMR (100 MHz, $CDCl_3$): δ 170.6, 156.4, 143.7, 143.5, 141.2, 135.7, 131.3, 127.8, 127.17, 127.15, 125.4, 125.2, 122.3, 120.2, 120.0, 119.1, 67.5, 53.1, 52.5, 50.0, 47.4, 46.9, 31.9, 29.98, 29.9, 29.7, 29.67, 29.62, 29.61, 29.5, 29.4, 29.39, 29.37, 29.0, 28.9, 26.3, 26.2, 25.9, 22.7, 14.1. MS (ESI) *m*/*z* 784.6 (M).

4.3.4. *N(α)-[(9H-Fluoren-9-ylmethoxy)carbonyl]-N(π)-(trans-dec-2-en-1-yl)-L-histidine methyl ester (**6**)*

Compound **6** was synthesized using general procedure I, Tf_2O (293 μL, 1.74 mmol), *trans*-2-decen-1-ol (324 μL, 1.74 mmol), histidine methyl ester **1** (1.00 g, 1.58 mmol), DIEA (303 μL, 1.74 mmol), TFA (1.21 mL, 15.78 mmol), and TIS (357 μL, 1.74 mmol). The crude product was purified by silica gel column chromatography (CH_2Cl_2/MeOH, from 100:1 to 20:1) to provide **6** (0.29 g, 35%) as a colorless gum.

^{1}H NMR (400 MHz, $CDCl_3$): δ 8.13 (s, 1H), 7.75 (d, 2H, *J* = 7.4 Hz), 7.56 (d, 2H, *J* = 7.4 Hz), 7.39 (t, 2H, *J* = 7.4 Hz), 7.30 (t, 2H, *J* = 7.4 Hz), 7.05 (s, 1H), 5.97 (m, 1H), 5.67 (m, 1H), 5.47 (m, 1H), 4.57–4.52 (m, 3H), 4.37 (m, 2H), 4.18 (t, 1H, *J* = 6.6 Hz), 3.75 (s, 3H), 3.18–3.13 (m, 2H), 2.02 (m, 2H), 1.34–1.24 (m, 10H), 0.87 (t, 3H, *J* = 6.6 Hz). ^{13}C NMR (100 MHz, $CDCl_3$): δ 170.9, 155.9, 143.6, 143.58, 141.3, 138.3, 135.7, 128.3, 127.8, 127.1, 125.0, 122.5, 122.0, 120.0, 67.2, 53.0, 52.9, 48.1, 47.0, 32.1, 31.7, 29.1, 29.0, 28.7, 26.4, 22.6, 14.1. MS (ESI) *m*/*z* 530.3 $(M + H)^+$.

4.4. *General procedure II for the hydrolysis of esters **7**–**11***

4.4.1. *N(α)-[(9H-Fluoren-9-ylmethoxy)carbonyl]-N(π), N(τ)-bis (heptyl)-L-histidine (**7**)*

To a solution of compound **2** (1.08 g, 1.83 mmol) in 1,4-dioxane (35 mL) was added 2 N HCl (35 mL) and refluxed for 10 h. The solvent was removed in vacuo, and the residue was partitioned between CH_2Cl_2 and H_2O. The organic layer was dried (Na_2SO_4) and evaporated in vacuo. The residue was purified by silica gel column chromatography (CH_2Cl_2/MeOH, from 20:1 to 5:1) to provide **7** (563 mg, 54%) as a colorless gum.

^{1}H NMR (400 MHz, $CDCl_3$): δ 8.86 (s, 1H), 7.73 (d, 2H, *J* = 7.1 Hz), 7.66–7.48 (m, 2H), 7.43–7.23 (m, 4H), 6.66 (s, 1H), 4.60 (m, 1H), 4.35–4.19 (m, 2H), 4.18–3.92 (m, 5H), 3.34–3.16 (m, 2H), 1.84–1.64 (m, 4H), 1.31–1.08 (m, 16H), 0.82 (t, 6H, *J* = 6.2 Hz). ^{13}C NMR (100 MHz, $CDCl_3$) δ 171.5, 156.2, 143.8, 143.3, 141.3, 141.2, 135.7, 130.9, 127.9, 127.24, 127.18, 125.3, 125.1, 122.0, 121.1, 120.0, 118.8, 67.1, 52.9, 50.1, 47.5, 46.9, 31.5, 30.1, 30.0, 28.6, 28.5, 26.2, 26.1, 22.4, 14.0. MS (ESI) *m*/*z* 574.3 (M).

4.4.2. *N(α)-[(9H-Fluoren-9-ylmethoxy)carbonyl]-N(π), N(τ)-bis (decyl)-L-histidine (**8**)*

Compound **8** was synthesized using general procedure II, compound **3** (500 mg, 0.74 mmol), 2 N HCl (10 mL), and 1,4-dioxane

(10 mL). The crude product was purified by silica gel column chromatography (CH_2Cl_2/MeOH, from 10:1 to 5:1) to provide **8** (242 mg, 50%) as a colorless gum.

^{1}H NMR (400 MHz, $CDCl_3$): δ 8.71 (s, 1H), 7.74 (d, 2H, J = 7.4 Hz), 7.58 (m, 2H), 7.38 (t, 2H, J = 7.4 Hz), 7.32–7.27 (m, 4H), 6.58 (d, 1H, J = 6.4 Hz), 4.53 (m, 1H), 4.34–4.24 (m, 2H), 4.13 (t, 1H, J = 7.3 Hz), 4.09–3.97 (m, 4H), 3.25 (m, 2H), 1.73 (br s, 4H), 1.26–1.19 (m, 28H), 0.86 (t, 6H, J = 6.5 Hz). ^{13}C NMR (100 MHz, $CDCl_3$): δ 172.1, 156.2, 143.8, 143.4, 141.3, 141.2, 135.0, 131.2, 127.8, 127.2, 125.3, 125.0, 122.1, 121.1, 120.0, 118.9, 67.3, 53.4, 49.9, 47.4, 46.9, 31.84, 31.82, 30.0, 29.95, 29.4, 29.38, 29.2, 29.0, 28.9, 26.3, 26.2, 22.6, 14.1. MS (ESI) m/z 658.5 (M).

4.4.3. N(α)-[(9H-Fluoren-9-ylmethoxy)carbonyl]-N(π)-(decyl)-L-histidine (**9**)

Compound **9** was synthesized using general procedure II, compound **4** (440 mg, 0.83 mmol), 2 N HCl (5 mL), and 1,4-dioxane (5 mL). The crude product was purified by silica gel column chromatography (CH_2Cl_2/MeOH, from 10:1 to 5:1) to provide **9** (270 mg, 63%) as a white solid.

^{1}H NMR (400 MHz, $CDCl_3$): δ 8.26 (s, 1H), 7.74 (d, 2H, J = 7.4 Hz), 7.57 (t, 2H, J = 7.4 Hz), 7.38 (t, 2H, J = 7.4 Hz), 7.28 (t, 2H, J = 7.4 Hz), 7.16 (s, 1H), 6.28 (br s, 1H), 4.44 (br s, 1H), 4.36 (m, 2H), 4.18 (t, 1H, J = 6.8 Hz), 3.98 (m, 2H), 3.27 (m, 2H), 1.69 (br s, 2H), 1.24 (br s, 14H), 0.86 (t, 3H, J = 6.7 Hz). ^{13}C NMR (100 MHz, $CDCl_3$): δ 173.6, 156.0, 143.9, 143.6, 141.3, 141.28, 133.5, 130.5, 127.8, 127.1, 125.1, 125.0, 120.0, 119.5, 67.0, 54.4, 47.1, 46.7, 31.8, 30.2, 29.4, 29.36, 29.2, 29.0, 26.4, 26.3, 22.6, 14.1. MS (ESI) m/z 518.3 $(M + H)^+$.

4.4.4. N(α)-[(9H-Fluoren-9-ylmethoxy)carbonyl]-N(π), N(τ)-bis(tetradecyl)-L-histidine (**10**)

Compound **10** was synthesized using general procedure II, compound **5** (1.34 g, 1.71 mmol), 2 N HCl (20 mL), and 1,4-dioxane (20 mL). The crude product was purified by silica gel column chromatography (CH_2Cl_2/MeOH, from 10:1 to 5:1) to provide **10** (610 mg, 46%) as a colorless gum.

^{1}H NMR (400 MHz, $CDCl_3$): δ 8.67 (s, 1H), 7.73 (d, 2H, J = 7.4 Hz), 7.58 (m, 2H), 7.38 (t, 2H, J = 7.4 Hz), 7.30–7.28 (m, 3H), 6.63 (br s, 1H), 4.55 (br s, 1H), 4.33–4.23 (m, 2H), 4.12 (t, 1H, J = 7.0 Hz), 4.09–4.00 (m, 4H), 3.25 (m, 2H), 1.71 (br s, 4H), 1.29–1.18 (m, 44H), 0.88 (t, 6H, J = 6.7 Hz). ^{13}C NMR (100 MHz, $CDCl_3$) δ 172.3, 156.2, 143.9, 143.4, 141.3, 141.2, 135.0, 131.1, 127.9, 127.8, 127.2, 125.3, 125.1, 122.0, 121.1, 120.0, 118.9, 67.3, 53.4, 49.9, 47.4, 46.9, 31.9, 30.0, 29.9, 29.7, 29.67, 29.63, 29.5, 29.4, 29.37, 29.0, 28.9, 26.3, 26.2, 22.7, 14.1. MS (ESI) m/z 770.6 (M).

4.4.5. N(α)-[(9H-Fluoren-9-ylmethoxy)carbonyl]-N(π)-(trans-dec-2-en-1-yl)-L-histidine (**11**)

Compound **11** was synthesized using general procedure II, compound **6** (170 mg, 0.32 mmol), 2 N HCl (3 mL), and 1,4-dioxane (3 mL). The crude product (155 mg, 94%) was obtained as a white solid and used without further purification in the following step.

^{1}H NMR (400 MHz, $CDCl_3$): δ 11.9 (br s, 1H), 8.28 (s, 1H), 7.74 (d, 2H, J = 7.4 Hz), 7.57 (m, 2H), 7.37 (t, 2H, J = 7.4 Hz), 7.28 (t, 2H, J = 7.4 Hz), 7.19 (s, 1H), 6.30 (br s, 1H), 5.69 (m, 1H), 5.42 (m, 1H), 4.57–4.47 (m, 3H), 4.37 (m, 2H), 4.16 (m, 1H), 3.26 (m, 2H), 1.97 (m, 2H), 1.26–1.21 (m, 10H), 0.86 (t, 3H, J = 6.6 Hz). ^{13}C NMR (100 MHz, $CDCl_3$): δ 173.4, 156.1, 143.8, 143.6, 141.3, 141.2, 139.4, 133.8, 130.5, 127.8, 127.1, 125.1, 121.2, 120.0, 119.4, 67.0, 54.2, 48.7, 47.1, 32.2, 31.7, 29.1, 29.0, 28.6, 26.3, 22.6, 14.1. MS (ESI) m/z 516.39 $(M + H)^+$.

4.5. General procedures for peptide synthesis

Rink amide 4-methylbenzhydrylamine (MBHA) resin and 9-fluorenylmethoxycarbonyl (Fmoc) amino acids were obtained from Calbiochem-Novabiochem (La Jolla, CA). Other reagents used for peptide synthesis included trifluoroacetic acid (TFA; Sigma–Aldrich), piperidine (Merck), *O*-benzotriazole-1-yl-*N*,*N*,*N*′,*N*′-tetramethyluronium hexafluorophosphate (HBTU; Sigma–Aldrich), 1-hydroxybenzotriazole (HOBt; Sigma–Aldrich) and *N*,*N*-dimethylformamide (DMF, peptide synthesis grade; Biolab). All other reagents were of analytical grade. The buffers were prepared in double glass-distilled water. All the HDLPs were prepared by Fmoc SPPS methods using Rink amide resin with an initial loading of 0.61 mmol/g, unless otherwise noted. Resins were swollen in DMF for 45 min prior to synthesis. For sequence extension, the Fmoc-Arg(Pbf)-OH (5.0 eq.) along with HBTU (5.0 eq.) and HOBt (5.0 eq.) was added to the free amine on resin in the presence of *N*,*N*-diisopropylethylamine (DIEA) (5.0 eq.) in 2 mL DMF and allowed to proceed for 1 h with Vortex stirring. After washing with DMF, Fmoc deprotection was achieved with 20% piperidine in DMF (1 × 10 min, 2 × 3 min). The resin was washed once again, and the process was repeated for the next amino acid and finally the resin was washed with DMF, methanol, dichloromethane and ether, and then dried under vacuum. Linear peptides were cleaved from the resin with 5% triisopropylsilane (TIS) and 5% H_2O in TFA (approximately 2 mL of TFA per 100 mg of resin) for 2 h. The cleavage mixture was mixed with cold ether to precipitate the peptide and then filtered. Purification of crude peptide was carried out on the preparative Vydac C_{18} column (15 μm, 20 mm × 250 mm) using an appropriate 10–90% water/acetonitrile gradient in the presence of 0.05% TFA (A: water buffer, B: acetonitrile buffer). The final purity of the HDLPs (>98%) was assessed by RP-HPLC on an analytical Vydac C_{18} column (4.6 mm × 250 mm, 300 Å, 5 μm particle size). The molecular masses of HDLPs were determined using matrix-assisted laser-desorption ionization-time-of-flight mass spectrometry (MALDI-TOF MS, Voyager-DE STR). MS (MALDI-TOF) m/z: HDLP **1**; 663.6 (M), HDLP **2**; 747.7 (M), HDLP **3**; 859.8 (M), HDLP **4**; 607.6 $(M + H)^+$, HDLP **5**; 605.6 $(M + H)^+$, HDLP **6**; 747.7 (M), HDLP **7**; 747.8 (M), HDLP **8**; 591.6 (M).

4.6. Antimicrobial activity (MIC)

The antimicrobial activity of the peptides against three Gram-positive bacterial strains and three Gram-negative bacterial strains was examined by using the broth microdilution method in sterile 96-well plates. Aliquots (100 μL) of a bacterial suspension at 2 × 10^6 colony-forming units (CFU)/mL in 1% peptone with 0 or 150 mM NaCl were added to 100 μL of the peptide solution (serial 2-fold dilutions in 1% peptone). After incubation for 18–20 h at 37 °C, bacterial growth inhibition was determined by measuring the absorbance at 600 nm with a Microplate Autoreader EL 800 (Bio-Tek Instruments, VT). The minimal inhibitory concentration (MIC) was defined as the minimum peptide concentration inhibited bacteria growth. Three types of Gram-positive bacteria (*B. subtilis* [KCTC 3068], *S. epidermidis* [KCTC 1917] and *S. aureus* [KCTC 1621]) and three types of Gram-negative bacteria (*E. coli* [KCTC 1682], *P. aeruginosa* [KCTC 1637] and *S. typhimurium* [KCTC 1926]) were procured from the Korean Collection for Type Cultures (KCTC) at the Korea Research Institute of Bioscience and Biotechnology (KRIBB). Methicillin-resistant *S. aureus* (MRSA) (CCARM 3089, CCARM 3090 and CCARM 3095) were obtained from the Culture Collection of Antibiotic-Resistant Microbes (CCARM) at Seoul Women's University (Seoul, Korea).

4.7. Hemolytic activity

Fresh human red blood cells (hRBCs) were centrifuged, washed three times with PBS, dispensed into 96-well plates as 100 mL of 4% (v/v) hRBC in PBS, and 100 mL of peptide solution was added to each well. Plates were incubated for 1 h at 37 °C, then centrifuged at 1000× *g* for 5 min. Samples (100 mL) of supernatant were transferred to 96-well plates and hemoglobin release was monitored by

measuring absorbance at 414 nm. Zero hemolysis was determined in PBS (A_{PBS}) and 100% hemolysis was determined in 0.1% (v/v) Triton X-100 (A_{triton}). The percentage hemolysis was calculated as: % hemolysis = $100 \times [(A_{sample} - A_{PBS})/(A_{triton} - A_{PBS})]$.

4.8. Proteolytic stability

E. coli (KCTC 1682) and *S. aureus* (KCTC 1621) were grown overnight for 18 h at 37 °C in 10 mL of LB broth and then 10 μL of this culture was inoculated into 10 mL of fresh LB and incubated for an additional 3 h at 37 °C to obtain mid-logarithmic phase organisms. Digestion of each peptide by trypsin was carried out using 50 μg/ml peptide and 0.2 μg/ml trypsin in 50 mM Tris–HCl buffer, pH 7.5 at 37 °C for 2 h. The reaction solution (50 μL) was added to 150 μL of a bacterial suspension (2×10^6 CFU/mL in 1% peptone). After incubation at 37 °C for 18–20 h, the bacterial growth inhibition was determined by measuring absorbance at 600 nm with a Microplate Autoreader EL 800 (Bio-Tek Instruments).

4.9. Morphological changes of bacteria upon HDLPs addition

Morphological changes of a Gram-negative bacterial strain (*E. coli* [KCTC 1682]) and a Gram-positive bacterial strain (*S. aureus* [KCTC 1621]) upon the addition of HDLPs and melittin were analyzed using transmission electron microscopy (TEM). Bacterial culture at 2×10^6 colony-forming units (CFU)/mL in LB media was washed 3 times in phosphate buffered saline (PBS) via a series of centrifugation at 10,000× *g*, for 5 min, and re-suspension. 100 μL of HDLPs in PBS was added to an equal volume of bacterial suspension to a final concentration at ×3 MIC. Following the addition of HDLPs, the samples were incubated for 1 h at 37 °C. Bacterial cell pellet after centrifugation was re-suspended in 20 μL PBS for TEM specimen preparation. 5 μL of sample solution was loaded onto a carbon film-coated TEM grid that was rendered hydrophilic by glow discharge. After 90 s, excess sample solution was washed off with distilled water. 5 μL of 1% uranyl acetate was loaded onto the grid for negative staining for 1 min, and excess stain solution was blotted using a piece of filter paper. Samples were imaged using a Tecnai G^2 Spirit electron microscope (FEI) equipped with lanthanum hexaboride (Lab_6) gun, operating at 120 kV. Images were recorded using Ultrascan 4000 charge-coupled device (CCD) camera (Gatan).

Acknowledgments

This work was supported in part by the Korea Basic Science Institute's research grant T33418 (J.K.B), T33518 (J-K Hyun), the National Cancer Institute's Intramural Research grant (K.S.L) and the Korea Research Foundation funded by the Korean Government (KRF-2011-0009039 to S.Y. Shin).

Appendix A. Supplementary data

Supplementary data related to this article can be found at http://dx.doi.org/10.1016/j.ejmech.2013.07.008.

References

[1] B. Findlay, G.G. Zhanel, F. Schweizer, Cationic amphiphiles, a new generation of antimicrobials inspired by the natural antimicrobial peptide scaffold, Antimicrob. Agents Chemother. 54 (2010) 4049–4058.
[2] G.G. Perron, M. Zasloff, G. Bell, Experimental evolution of resistance to an antimicrobial peptide, Proc. Biol. Sci. 273 (2006) 251–256.
[3] A.T. Yeung, S.L. Gellatly, R.E. Hancock, Multifunctional cationic host defence peptides and their clinical applications, Cell. Mol. Life Sci. 68 (2011) 2161–2176.
[4] H. Tsubery, I. Ofek, S. Cohen, M. Fridkin, N-Terminal modifications of Polymyxin B nonapeptide and their effect on antibacterial activity, Peptides 22 (2001) 1675–1681.
[5] J.N. Steenbergen, J. Alder, G.M. Thorne, F.P. Tally, Daptomycin: a lipopeptide antibiotic for the treatment of serious Gram-positive infections, J. Antimicrob. Chemother. 55 (2005) 283–288.
[6] N.P. Chongsiriwatana, T.M. Miller, M. Wetzler, S. Vakulenko, A.J. Karlsson, S.P. Palecek, S. Mobashery, A.E. Barron, Short alkylated peptoid mimics of antimicrobial lipopeptides, Antimicrob. Agents Chemother. 55 (2011) 417–420.
[7] D. Avrahami, Y. Shai, Bestowing antifungal and antibacterial activities by lipophilic acid conjugation to D, L-amino acid-containing antimicrobial peptides: a plausible mode of action, Biochemistry 42 (2003) 14946–14956.
[8] A. Majerle, J. Kidric, R. Jerala, Enhancement of antibacterial and lipopolysaccharide binding activities of a human lactoferrin peptide fragment by the addition of acyl chain, J. Antimicrob. Chemother. 51 (2003) 1159–1165.
[9] P. Mak, J. Pohl, A. Dubin, M.S. Reed, S.E. Bowers, M.T. Fallon, W.M. Shafer, The increased bactericidal activity of a fatty acid-modified synthetic antimicrobial peptide of human cathepsin G correlates with its enhanced capacity to interact with model membranes, Int. J. Antimicrob. Agents 21 (2003) 13–19.
[10] N.A. Lockwood, J.R. Haseman, M.V. Tirrell, K.H. Mayo, Acylation of SC4 dodecapeptide increases bacterial potency against Gram-positive bacterial, including drug resistant strains, Biochem. J. 378 (2004) 93–103.
[11] A. Makovitzki, D. Avrahami, Y. Shai, Ultrashort antibacterial and antifungal lipopeptides, Proc. Natl. Acad. Sci. U. S. A. 103 (2006) 15997–16002.
[12] A. Makovitzki, J. Baram, Y. Shai, Antimicrobial lipopolypeptides composed of palmitoyl di- and tricationic peptides: in vitro and in vivo activities, self-assembly to nanostructures, and a plausible mode of action, Biochemistry 47 (2008) 10630–10636.
[13] A.F. Chu-Kung, K.N. Bozzelli, N.A. Lockwood, J.R. Haseman, K.H. Mayo, M. Tirrell, Promotion of peptide antimicrobial activity by fatty acid conjugation, Bioconjug. Chem. 15 (2004) 530–535.
[14] G. Laverty, M. McLaughlin, C. Shaw, S.P. Gorman, B.F. Gilmore, Antimicrobial activity of short, synthetic cationic lipopeptides, Chem. Biol. Drug Des. 75 (2010) 563–569.
[15] C.J. Arnusch, H.B. Albada, M. Van Vaardegem, R.M.J. Liskamp, H.-G. Sahl, Y. Shadkchan, N. Osherov, Y. Shai, Trivalent ultrashort lipopeptides are potent pH dependent antifungal agents, J. Med. Chem. 55 (2012) 1296–1302.
[16] A. Tossi, L. Sandri, A. Giangaspero, Amphipathic, alpha-helical antimicrobial peptides, Biopolymers 55 (2000) 4–30.
[17] N.K. Brogden, K.A. Brogden, Will new generations of modified antimicrobial peptides improve their potential as pharmaceuticals? Int. J. Antimicrob. Agents 38 (2011) 217–225.
[18] J. Pernak, J. Rogoza, I. Mirska, Synthesis and antimicrobial activities of new pyridinium and benzimidazolium chlorides, Eur. J. Med. Chem. 36 (2001) 313–320.
[19] H. Turkmen, N. Ceyhan, N. Ulku Karabay Yavasoglu, G. Ozdemir, B. Cetinkaya, Synthesis and antimicrobial activities of hexahydroimidazo[1,5-*a*]pyridinium bromides with varying benzyl substituents, Eur. J. Med. Chem. 46 (2011) 2895–2900.
[20] V. Sambhy, B.R. Peterson, A. Sen, Antibacterial and hemolytic activities of pyridinium polymers as a function of the spatial relationship between the positive charge and the pendant alkyl tail, Angew. Chem. Int. Ed. 47 (2008) 1250–1254.
[21] L. Kardas-Sloma, P.Y. Boelle, L. Opatowski, C. Brun-Buisson, D. Guillemot, L. Temime, Impact of antibiotic exposure patterns on selection of community-associated methicillin-resistant Staphylococcus aureus in hospital settings, Antimicrob. Agents Chemother. 55 (2011) 4888–4895.
[22] D. Takahashi, S.K. Shukla, O. Prakash, G. Zhang, Structural determinants of host defense peptides for antimicrobial activity and target cell selectivity, Biochimie 92 (2010) 1236–1241.
[23] J. Svenson, W. Stensen, B.O. Brandsdal, B.E. Haug, J. Monrad, J.S. Svendsen, Antimicrobial peptides with stability toward tryptic degradation, Biochemistry 47 (2008) 3777–3788.
[24] W. Qian, F. Liu, T.R. Burke Jr., Investigation of unanticipated alkylation at the N (π) position of a histidyl residue under Mitsunobu conditions and synthesis of orthogonally protected histidine analogues, J. Org. Chem. 76 (2011) 8885–8890.